ChemPubSoc Europe

DOI: 10.1002/slct.201901001

Chemistry SELECT Full Papers

Materials Science inc. Nanomaterials & Polymers

Antibacterial Properties of Charged TiN Surfaces for Dental Implant Application

Patrick H. Carey IV,[a] Fan Ren,[a] Ziqi Jia,[b] Christopher D Batich,[b] Samira E. A. Camargo,[c] Arthur E. Clark,[c] Valentin Craciun,[d] Daniel W. Neal,[e] and Josephine F. Esquivel-Upshaw*[c]

The formation and characterization of positively surface charged TiN surfaces were investigated for improving dental implant survival. Surface nitrogen atoms of a traditional TiN implant were converted to a positive charge by a quaternization reaction which greatly increased the antibacterial efficiency. Ti, TiN, and quaternized TiN samples were incubated with human patient subgingival bacteria for 4 hours at 37 °C in an anaerobic environment with an approximate 40% reduction in counts on the quaternized surface over traditional Ti and TiN. The samples were challenged with *Streptococcus Mutans* and fluorescent imaging confirmed significant reduction in the quaternized TiN over the traditional Ti and TiN. Contact angle measurement and X-Ray Photoelectron Spectroscopy (XPS) were utilized to confirm the surface chemistry changes. The XPS results found the charged quaternized nitrogen peak at 399.75 eV that is unique to the quaternized sample.

Introduction

Approximately 5% of all dental implants anchored by osseointegration will fail within 10 years.[1] A primary culprit for implant failure is peri-implantitis, which is site specific bacterial infection leading to bone loss around the implant and soft tissue inflammation. Controlling the inflammation through improved hygiene by reducing microbial activity is the only current method to combat potential implant failure, as there is no conclusive treatment to stop infection and progression of the disease.[2] Anywhere from 10% to 45% of all dental implants will have detectable peri-implantitis inflammatory reactions. Characterizing peri-implantitis has proven to be difficult due to many factors such as patients' dental history, medical conditions, hygiene and eating habits.[3] For example, patients with previous history of periodontal disease have lower implant survival rates, but diseases such as osteoporosis or diabetes have not demonstrated consistent effects.[2a,b]

In addition, the bacterial flora has been explored to determine a prevalence of certain bacteria which may lend to formation of peri-implantitis. The sub-gingival flora of sites with peri-implantitis have similar flora to that of periodontitis with mostly gram-negative bacteria.[4] *Persson et al.* identified 19 bacterial species with higher counts at the site of peri-implantitis infection than at implant sites without infection, with seven bacteria strains accounting for 30% of bacterial flora at the infection site as compared to 14% at non-infected implants.[4a] These results indiciate that peri-implantitis may not directly result from a singular bacteria strain infecting the implant site, rather an imbalance of a healthy flora.

Use of antibacterial coatings may provide a method for improving implant lifetime. Even use of different metals in an implant has significant effect on bacterial growth. Titanium nitride (TiN) is the most promising metal as this promotes osseointegration while also having lower bacterial growth rate than traditional titanium (Ti) implants.[5] Current implants utilize several microns thick TiN by plasma spraying coatings on implant surfaces. Despite this, peri-implantitis still exists with these types of implants. Many groups have explored addition of metallic particles to the implant such as copper, silver, and metal oxides;[6] however, a galvanic effect was reported where patients who had gold or amalgam in their teeth concurrently with Ti implants displayed yellow nails and were found to have Ti in their nail clippings.[7] Thus, the additional metallic elements in Ti may enhance Ti and other metals to dissolve into the bodily environment. Primarily, the impact of metal dissolution into the surrounding tissue may facilitate peri-implant inflammatory reactions.[8]

Molecules with quaternary nitrogen atoms have shown the ability to disrupt the cell wall, leading to leakage of the cell contents and eventual apoptosis of the bacteria.[9] To minimize concerns over dissolute metallic species undergoing unfavorable interactions with the surrounding tissues, modifying the nitrogen atoms on TiN surface into quaternary nitrogen atoms may be a better alternative to inhibit peri-implant inflammatory reactions.

[a] *P. H. Carey IV, Dr. F. Ren*
Department of Chemical Engineering, University of Florida, Gainesville, FL
[b] *Z. Jia, Dr. C. D Batich*
Department of Materials Science and Engineering, University of Florida, Gainesville, FL
[c] *Dr. S. E. A. Camargo, Dr. A. E. Clark, Dr. J. F. Esquivel-Upshaw*
Restorative Dental Sciences, Division of Prosthodontics University of Florida, Gainesville, FLTel.: 352–273-6928
E-mail: jesquivel@dental.ufl.edu
[d] *Dr. V. Craciun*
National Institute for Lasers, Plasma and Radiation Physics, Magurele-Ilfov, Romania, and DENTIX MILLENNIUM SRL, Sabareni-Ilfov, Romania
[e] *D. W. Neal*
Department of Neurosurgery, University of Florida, Gainesville, FL

Supporting information for this article is available on the WWW under https://doi.org/10.1002/slct.201901001

In this study, we aim to test the effectiveness of quaternized TiN on reducing bio-film growth by employing allyl bromide through the Menschutkin reaction to convert nitrogen atoms on the TiN surface into quaternary nitrogen. Sessile drop contact angle and x-ray photoelectron spectroscopy (XPS) were employed to confirm the nitrogen atoms were converted into quaternary nitrogen. The objectives of this study are to test the hypotheses that: (1) quaternized TiN will have greater anti-bacterial properties compared with Ti and TiN as a function of colony forming units and (2) bacterial film thickness will affect the anti-microbial properties of these coatings.

Results

ANOVA ($R2 = .288$, adjusted $R2 = .250$, F statistic $= 7.6$ on 5 and 94 degrees of freedom) revealed that coating material is significantly associated with bacteria level ($p < .0001$). Pairwise comparisons among material groups show that across all thicknesses: (1) Quaternized TiN (Q) is significantly lower than Titanium (T) ($p < .0001$) and for any random thickness or experimental run, Q is estimated to be 45.6 units lower than T (95% CI = [-65.0, −26.2]); (2) Q is significantly lower than Titanium nitride (N) ($p = .0003$) and for any random thickness or experimental run, Q is estimated to be 37.1 units lower than N (95% CI = [-56.8, −17.4]); (3) T and N are not significantly different ($p = .392$) (Figure 1).

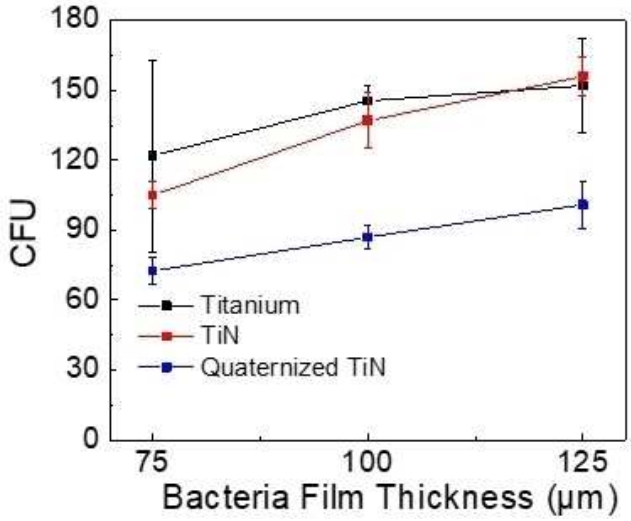

Figure 1. Colony forming unit (CFU) of bacteria growth plotted for Ti, TiN or quaternized TiN substrate and different film thicknesses.

Bacteria thickness is significantly associated with bacteria level ($p = .002$). Pairwise comparisons among thickness groups show that across all materials: (1) 100 μm yields marginally higher values than 75 μm ($p = .060$), and for any random material and experimental run, 100 μm is estimated to be 18.9 units higher than 75 μm (95% CI = [-0.778, 38.6]); (2) 125 μm yields significantly higher values than 75 μm ($p = .0004$) and for any random material and experimental run, 125 μm is estimated to be 38.2 units higher than 75 (95% CI = [16.6, 55.7]); (3) 125 μm yields marginally higher values than 100 ($p = .082$) and for any random material and experimental run, 125 μm is estimated to be 17.3 units higher than 100 (95% CI = [-2.24, 38.8]) (Figure 2). The interaction between coating material and bacterial thickness is $p = 0.977$ indicating that the anti-bacterial effectiveness of the coatings is not expected to be affected by the thickness of bacteria. Experimental run was not associated with bacteria level ($p = .450$).

The result from the staining assay shows a significant reduction in the number of live bacteria, on the quaternized TiN samples, as shown by the fluorescence images on Figure 2. The calculation of live bacteria coverage indicate the bactericidal effect of the quaternized TiN samples against *S. mutans* after 4 h of culture, significantly decreased the number of live bacteria (Figure 4).

Pairwise comparisons among material groups show regard to live bacteria coverage: (1) Quaternized TiN (Q) (10.85%) is significantly lower than Titanium (T) (89.1%) ($p = < .0001$); (2) Q is significantly lower than Titanium nitride (N) (82.2%) ($p < .0001$); (3) T and N are not significantly different ($p = .312$) (Figure 3).

Sessile contact angle measurement images of part of a single water droplet placed on Ti, TiN or quaternized TiN surface are shown in Figure 4. For both Ti and TiN substrates, a small contact angle was observed indicating that Ti and TiN surface were hydrophilic and had good wettability (Figure 3). On the contrary, a larger contact angle was obtained on the quaternized TiN surface. Table 1 lists the specific average contact angles and standard deviations of Ti, TiN and quaternized TiN substrates. The average contact angle measurements were 12° for Ti; 16° for TiN and 67° for quaternized TiN substrates. zeta potential measurements were used to characterize the change in surface charge density of the samples. Surface charge density measurements were taken in a slightly acidic solution of pH 5.5. As deposited TiN and quaternized TiN exhibited surface charge densities of 1.19×10^{-7} C/cm^2 and 1.81×10^{-7} C/cm^2, respectively.

Table 1. Sessile contact angle measurements performed on Ti, TiN and quaternized TiN substrate

Sample	Contact Angle (°)
Titanium after H_2O_2 clean	12 ± 2
TiN after clean	< 6
TiN in solvent 120 mins (no reagent)	16 ± 2
TiN Quaternization 30 mins	67 ± 1
TiN Quaternization 60 mins	72 ± 3
TiN Quaternization 120 mins	71 ± 2

The stacked XPS survey scans of the TiN surface and the quaternized TiN surface are shown in Figure 5a. The spectra were aligned through the presence of adventitious carbon peak at 284.8 eV from the atmospheric exposure during handling and transport between deposition tools. The general

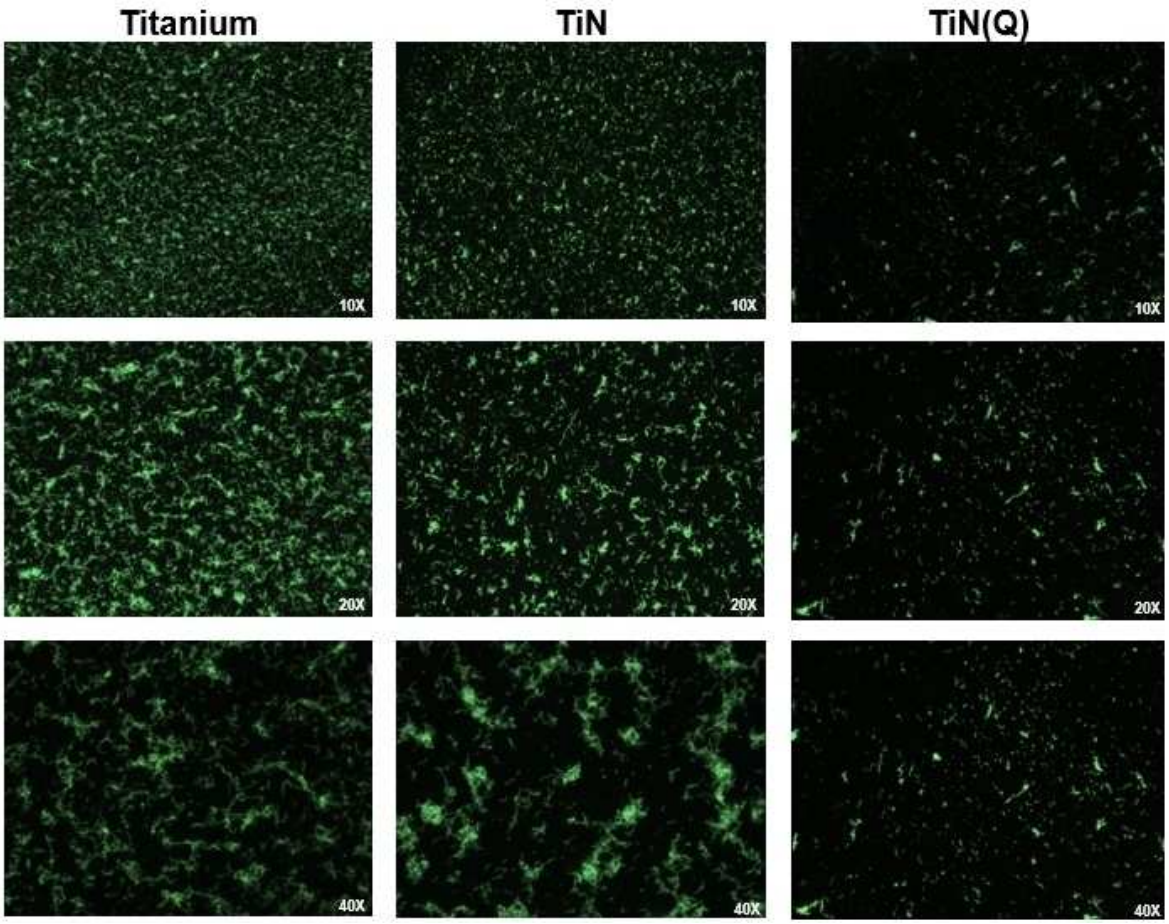

Figure 2. Fluorescence microscopy images of *S. mutans* cultured for 4 h on Ti, TiN or quaternized TiN substrate.

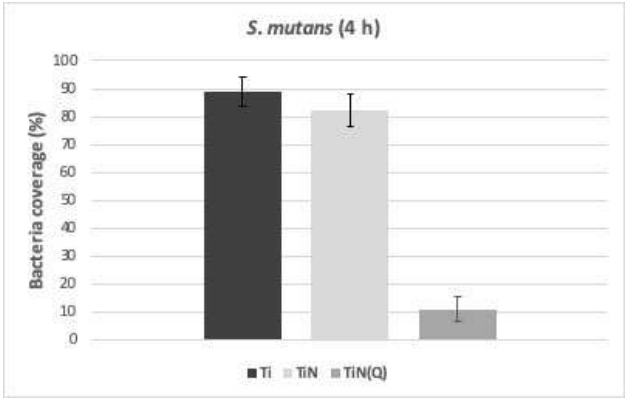

Figure 3. Live bacteria coverage of *S. mutans* cultured for 4 h on Ti, TiN or quaternized TiN substrate.

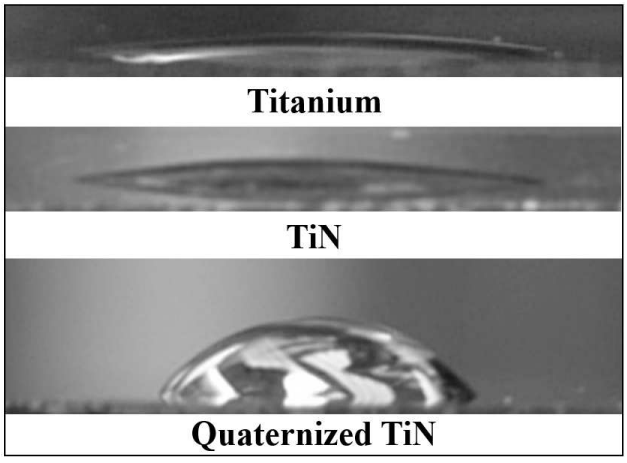

Figure 4. Contact angle images of Ti, TiN and quaternized TiN surface.

surface chemistry between the two samples is similar as only Ti, O, N, and C were identified in both samples.

The Nitrogen 1 s spectra acquired at different tilting angles for TiN and quaternized TiN sample are shown for 0° (Figure 5b) and 50° (Figure 5c). The main N peak corresponding to Ti–N bonds is located at 396.75 eV and there is an N satellite peak at 398.48 eV. The quaternized nitrogen, N^+, peak is 399.75 eV. As compared to the 0° spectra, surface effects are more pronounced for the tilted spectra, and the penetration depth of the x-ray source is greatly reduced.

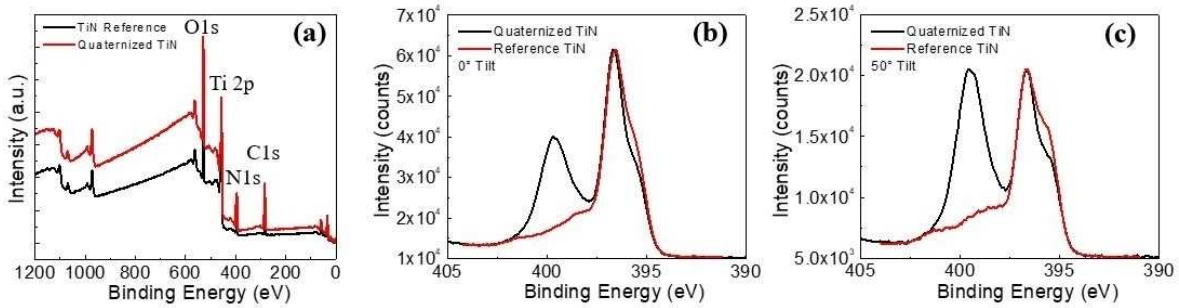

Figure 5. (a) Stacked XPS survey scans of reference TiN and quaternized TiN surface, (b) 0°, and (c) 50° tilted high resolution nitrogen 1 s XPS spectra of TiN and quaternized TiN surface.

Discussion

Confirmation of Surface Reaction

The integration and longevity of a dental implant requires the interface between bone and implant remain bacteria free. TiN has been shown to greatly improve development of bone around an implant and decrease the bacteria count over Ti implants.[5] Prior to evaluating the effectiveness of quaternized TiN on biofilm reduction, the success of converting surface bound nitrogen from uncharged to positively charged nitrogen needs to be verified. As shown in Figure 4 and Table I, the contact angles of Ti and TiN substrates were very low. The titanium sample after treatment with hydrogen peroxide was expected to be very hydrophilic because of the presence of Ti-O–H and Ti=O on Ti surface. The TiN sample was also very hydrophilic owing to the high polarity of TiN and the ability for hydrogen bonding of the water droplet to the nitrogen rich surface of TiN. For the quaternized TiN surface, surface nitrogen was converted into a positively charged nitrogen through the Menschutkin reaction and the contact angle should be low. However, as shown in Figure 4 and Table I, the contact angle of the quaternized TiN surface dramatically increased from 16 to 67°. This increase in hydrophobicity is due to the carbon chains extending from the surface bound nitrogen, as illustrated in equation (1) and Figure 3.

$$TiN + C_3H_5Br \rightarrow TiN^{+}(C_4H_5)_2 + Br^{-} \quad (1)$$

Menschutkin reactions are known to progress very rapidly due to the lower enthalpy of formation of higher substituted amines, which is evident by the reaction saturating within an hour. Hence the Menschutkin reaction is well suited for formation of quaternary ammonium salts and is difficult to stop at secondary or tertiary products.[10]

XPS surface analysis was employed to further confirm and identify changes in surface chemistry of quaternized TiN surface. As shown in Figure 6, the wide range analyses were acquired from the surface of the TiN and quaternized TiN substrates and Ti, O, N and C were the only elements identified on these two samples. This indicates that the general surface chemistry of TiN and quaternized TiN samples are identical. Therefore, a detailed peak analysis was necessary for confirmation of the surface reaction. High resolution XPS spectra of the N 1s regions were acquired at 0 (Figure 6b) and 50° (Figure 6c) angle with respect to the normal for the TiN and quaternized TiN surface. The main N peak corresponding to Ti–N bonds was located at 396.75 eV and there was an N satellite peak at 398.48 eV. The shoulder peak of N for Ti–N at 394.5 eV was resultant of N on N–Ti-O. The XPS peak[11] for quaternized nitrogen bound to the allyl group (-CH_3CH_5), N^+, was 399.75 eV. Surface effects were more pronounced for the spectra taken at a 50° tilt and the penetration depth of the x-ray source was greatly reduced, compared with the 0° spectra. For the N spectra of TiN substrate, the peak corresponding to the N of N–Ti-O was more pronounced because of the presence of oxide on the TiN surface. For the N 1s spectra of the quaternized nitrogen, this effect was evident in the increased relative intensity of the quaternized nitrogen peak at 399.75 eV compared with the TiN peak at 396.5 eV at 50°; indicating that N^+ atoms are situated on the surface of quaternized TiN. In addition, after a gentle sputtering with 500 eV Ar ions for 30 seconds to remove the top atomic layers of the quaternized TiN substrate, the quaternized nitrogen peak had completely disappeared. This also confirmed that quaternized nitrogen only exists on the top surface of the quaternized TiN substrate.

Impact of Quaternized TiN Surface on Biofilm Growth

As previously stated, the oral microbiome is incredibly diverse, and no singular bacteria has been identified as the primary causating agent of peri-implantitis. Thus, preventing all types of microbial growth near the implant site may provide the best avenue for implant survival. The variance experienced with efficacy is expected as each patient's flora will vary day-to-day and may respond differently depending on environmental factors such as diet, hygiene, periodontal condition, etc.

This study shows the potential anti-microbial effect of quaternized TiN compared with Ti and TiN at reducing CFUs (Figure 2) and bacteria coverage (Figure 3). The antibacterial mechanism of quaternized nitrogen has been proposed to interact with the cell wall, destroy the cytoplasmic membrane leading to the leakage of intracellular components and consequent cell death.[12] The quaternized surface outperformed both the TiN and Ti surfaces significantly within the

short 4-hour testing period for bacteria film thickness of 75 μm. Even with thick bacteria films that are 125 μm thick, the quaternized surfaces still significantly reduced bacterial counts compared with the other two substrates, indicating that the surface has the ability to neutralize bacteria that are not directly in contact with the surface. The lack of statistical significance in interaction between coating type and thickness indicates that the superior anti-bacterial properties of quaternized TiN versus TiN and Ti is evident across different thicknesses of bacteria. Also, the fluorescent images showed the proliferation of live bacteria was lower in quaternized TiN compared to Ti and TiN. Implant surfaces should have the ability to affect bacteria that is not only in direct contact with the surface but also in the immediate vicinity. This is because during the process of osseointegration, the implant will initially be surrounded by saliva and soft tissue. Additionally, failure of an implant will be induced by an infection beginning near the soft tissue which will propagate downward towards the base of the implant. However, with the quaternized surface that propagation can be hindered or completely prevented.

Conclusion

A novel application of the well-known Menschutkin reaction has been applied to convert the surface nitrogen of a TiN coated implant from neutral to positively charged. The surface change was monitored and confirmed by Sessile contact angle and XPS measurements. Biofilm growth noted a 40–50% reduction in bacteria over traditional implant surfaces within 4 hours and noticeable effects many microns away. Considering current technology and other works pursuing high biocidal activity for implant structures, this methodology provides a simple method that would require little manufacturing line changes to accommodate and bring to market.

Supporting Information Summary

Supporting information PDF contains experimental processes for fabrication of all sample types and details the characterization methodology used for each different section of the manuscript.

Acknowledgements

NIH-NIDCR Grant R01 DE025001 supported this study. Ceramic materials were supplied by Ivoclar Vivadent. Dektak was performed at the Nanoparticle Research Facility at the University of Florida. The XPS study was supported by a grant financed in the framework of Competitiveness Operational Program 2014–2020, ANCSI/MFE, project number MIFID ID P_39_366 Cod MySMIS 104809 and INFLPR Program NUCLEU-LAPLAS V.

Conflict of Interest

US provisional patent (US2019/044556) in place for quaternized TiN

Keywords: antibiotics · quaternary · Titanium · peri-implantitis · Menschutkin

[1] a) A. Mombelli, N. Müller, N. Cionca, *Clin Oral Implants Res* **2012**, *23*, 67–76; b) J. Lindhe, M. J. J. Clin, *Periodontol.* **2008**, *35*, 282–285; c) A. Mombelli, N. Cionca, *Clin Oral Implants Res* **2006**, *17*, 97–103.

[2] a) S. H. Safii, R. M. Palmer, R. F. Wilson, *Clin Implant Dent Relat Res* **2010**, *12*, 165–174; b) J. Prathapachandran, N. Suresh, *Dent. Res. J.* **2012**, *9*, 516–521; c) R. P. Teles, *Evidence Based Dentistry* **2003**, *4*, 88; d) S. Renvert, A.-M. Roos-Jansåker, N. Claffey, *J. Clin. Periodontol.* **2008**, *35*, 305–315; e) N. Claffey, E. Clarke, I. Polyzois and S. Renvert, *J. Clin. Periodontol.* **2008**, *35*, 316–332; f) M. Quirynen, M. Abarca, N. Van Assche, M. Nevins, D. Van Steenberghe, *J. Clin. Periodontol.* **2007**, *34*, 805–815; g) A. Mombelli, N. P. Lang, *Clin Oral Implants Res* **1992**, *3*, 162–168; h) N. Claffey and J. Egelberg, *J. Clin. Periodontol.* **1995**, *22*, 690–696.

[3] M. Godoy-Gallardo, M. C. Manzanares-Céspedes, P. Sevilla, J. Nart, N. Manzanares, J. M. Manero, F. J. Gil, S. K. Boyd, D. Rodríguez, *Mater. Sci. Eng.: C* **2016**, *69*, 538–545.

[4] a) A. Mombelli, F. Décaillet, *J. Clin. Periodontol.* **2011**, *38*, 203–213; b) G. R. Persson, S. Renvert, *Clin Implant Dent Relat Res* **2014**, *16*, 783–793; c) A. Mombelli, M. A. C. Oosten, E. Schürch, N. P. Lang, *Oral Microbiol. Immunol.* **1987**, *2*, 145–151.

[5] a) C. W. Berry, M. T. J. S. J. A. C. A. Henry, M. J. Wagner, *Implant Dent* **1992**, *1*; b) R. P. van Hove, I. N. Sierevelt, B. J. van Royen, P. A. Nolte, *BioMed Res. Int.* **2015**, *2015*, 9.

[6] a) R. Pokrowiecki, T. Zaręba, B. Szaraniec, K. Pałka, A. Mielczarek, E. Menaszek, S. Tyski, *Int. J. Nanomed.* **2017**, *12*, 4285–4297; b) R. Liu, K. Memarzadeh, B. Chang, Y. Zhang, Z. Ma, R. P. Allaker, L. Ren, K. Yang, *Sci. Rep.* **2016**, *6*, 29985; c) M. A. Vargas-Reus, K. Memarzadeh, J. Huang, G. G. Ren, R. P. Allaker, *Int. J. Antimicrob. Agents* **2012**, *40*, 135–139; d) R. P. Allaker, *J. Dent. Res.* **2010**, *89*, 1175–1186.

[7] F. Berglund, B. Carlmark, *Biol. Trace Elem. Res.* **2011**, *143*, 1–7.

[8] a) X. Li, P. Gao, P. Wan, Y. Pei, L. Shi, B. Fan, C. Shen, X. Xiao, K. Yang Z. Guo, *Sci. Rep.* **2017**, *7*, 40755; b) F. Khosravi, H. Mansouri-Torshizi, *J. Biomol. Struct. Dyn.* **2018**, *36*, 512–531; c) G. Li, Q.-m. Zhao, H.-l. Yang, L. Cheng, *Mater Res* **2016**, *19*, 735–740; d) S. Mei, H. Wang, W. Wang, L. Tong, H. Pan, C. Ruan, Q. Ma, M. Liu, H. Yang, L. Zhang, Y. Cheng, Y. Zhang, L. Zhao, P. K. Chu, *Biomaterials* **2014**, *35*, 4255–4265; e) R. Liu, Y. Tang, L. Zeng, Y. Zhao, Z. Ma, Z. Sun, L. Xiang, L. Ren, K. Yang, *Dent. Mater.* **2018**, *34*, 1112–1126.

[9] a) Y. Xue, H. Xiao, Y. Zhang, *Int. J. Mol. Sci.* **2015**, *16*, 3626; b) L. Timofeeva, N. Kleshcheva, *Appl. Microbiol. Biotechnol.* **2011**, *89*, 475–492; c) M. S. Hassan, H. M. M. Ibrahim, *Polym. Adv. Technol.* **2016**, *27*, 532–541; d) J. J. H. Oosterhof, K. J. D. A. Buijssen, H. J. Busscher, B. F. A. M. van der Laan, H. C. van der Mei, *Appl. Environ. Microbiol.* **2006**, *72*, 3673–3677.

[10] a) M. Smith, March, J., *March's Advanced Organic Chemistry: Reactions, Mechanisms, and Structure 6th ed*, John Wiley & Sons, Inc, Hoboken, NJ, **2007**, p; b) M. Harfenist, *J. Am. Chem. Soc.* **1957**, *79*, 4356–4358; c) K. J. Stanger, J.-J. Lee, B. D. Smith, *J Org Chem* **2007**, *72*, 9663–9668; d) N. Menschutkin, *Zeitschrift für Physikalische Chemie* **1890**, *6*, 1.

[11] a) D. Craciun, G. Socol, N. Stefan, G. Dorcioman, M. Hanna, C. R. Taylor, E. Lambers, V. Craciun, *Appl. Surf. Sci.* **2014**, *302*, 124–128; b) D. Jaeger and J. Patscheider, *J. Electron Spectrosc. Relat. Phenom.* **2012**, *185*, 523–534.

[12] a) J. Haldar, P. Kondaiah, S. Bhattacharya, *J. Med. Chem.* **2005**, *48*, 3823–3831; b) L.-A. B. Rawlinson, S. M. Ryan, G. Mantovani, J. A. Syrett, D. M. Haddleton, D. J. Brayden, *Biomacromolecules* **2010**, *11*, 443–453.

Submitted: March 18, 2019
Accepted: August 1, 2019